Investigating the Effect of Blood Dielectric Changes in Human Tissue Model by a Microwave Sensor

Moein Navaei[1] and Pejman Rezaei[1*]

***Abstract*— In this article, an original microwave sensor is presented which can detect the dielectric changes in the body tissue layer. The proposed sensor is created in the form of a microstrip structure and consists of U-shaped, interdigital, and waterfall parts. When the sensor is placed on a live sample, it can detect the dielectric changes that occur in the tissue layer. For this, a resonance is formed in the free load sensor at the frequency of 3.2 GHz then when the sample touches the sensor, according to the amount of relative dielectric changes of the tissue sample, the sensor resonant frequency is shifted. Considering that diseases related to glucose depend on blood, the purpose of sensing in the target sensor is the third layer of the modeled finger, i.e. blood. Therefore, the obtained results showed that the quality factor and sensitivity are 5346 and 0.5%, respectively.**

***Index Terms*— Microwave sensor; Quality factor; Multi-layer phantom; Human tissue; Sensitivity.**

I. INTRODUCTION

Blood sugar is one of the common diseases because this disease depends on the blood and changes in the blood cause an obvious change in the permittivity level of the blood [1, 2]. This paper examines the dielectric changes of blood, which is located in the third layer of body tissue. Blood glucose measurement methods can be invasive or non-invasive [3,4]. Using non-invasive methods to examine the internal parts of human tissue has been one of the important tasks of researchers. Research on blood glucose, fat, minerals, and proteins is of great importance in medical sciences. Considering that the speed of science has intensified in the new century, it has tried to use measurement methods that have high accuracy and speed, and non-invasive methods increase the speed of measurement [5, 6].

Microwave sensors are widely used in the medical and food industries, including its application in the food industry, it is possible to quickly detect food spoilage and determine the type of material [7, 8], and one of its important applications in the medical industry is determining blood glucose levels, which can be done by invasive and non-invasive methods [9].

Some technologies including optical [10], transdermal techniques [11], thermal spectrum measurement [12], breath acetone analysis [13], impedance spectroscopy [14], saliva analysis [15], graphene-based nanosensors [16], electrochemical methods [17], sweat and interstitial fluid (ISF) [18], contact lenses [19], acoustic spectroscopy [20], Raman spectroscopy [21], or a combination of these techniques [22] have been suggested for non-invasive monitoring of glucose [23-25].

Recently, interest in the characterization of the EM materials parameters for various applications in different fields, including medicine, health care, agriculture, chemistry, industry, and so on, has augmented dramatically. Equipment and sensors based on millimeter wave and microwave recognition techniques have attracted extensive attention, due to their being non-invasive, label-free, affordable, portable, and with the capability to integrate with extra portions of an intelligent system [26-28]. Numerous methods for EM properties measuring based on millimeter waves and microwaves have been proposed, which can be classified as non-resonant (broadband) [29-31] and resonant (narrow band) [32, 33] techniques. Among these ways, resonant techniques have become more general, especially for applications that need high sensitivity, accuracy, and speed in detection [34, 35].

One of the techniques to increase the EM parameters accuracy of materials is to use microwave resonance sensors, because a broader frequency range can be covered to measure the EM parameters of desired materials and achieve more comprehensive data about the sample under test (SUT) EM specifications [36]. Numerous research has been conducted in the field of various methods of measuring EM characteristics in the human tissue field; for example, split ring resonators (SRR) [37, 38] and complementary SRR (CSRR) [39], antennas [40, 41] and filters, transmission lines [42] and coaxial [43], implantable devices [44], and more can be mentioned [45].

One of the methods used in the field of sensor design is the optical method. The techniques used in it include

1: Electrical and Computer Engineering Faculty, Semnan University, Semnan, Iran.

Corresponding author: prezaei@semnan.ac.ir

plasmonic [46] or crystal structures that are used to identify cancer cells [47] or dielectric changes of materials [48].

Many sensor has been planned with a filter variety. The use of bandpass and bandstop filters is one of the common approaches that are used, and the parameters of return loss and insertion loss are usually used in the case of resonant sensors [49].

In this article, a microwave sensor with a resonance frequency of 3.2 GHz is designed. Then a model of human tissue including skin, fat, blood, and bone layers is presented. In the simulation with CST software, it is shown that when the sensor contacts the tissue model, its resonance frequency is shifted. The results have shown that the suggested biosensor has a Quality factor of 5346 with an appropriate sensitivity of 0.5%.

II. HUMAN TISSUE MODEL

Human tissue consists of different parts that are common to all humans. These parts include skin, fat, blood, and bone. These parts will have different characteristics for different people in different situations. For example, gender, age, and genetics are factors that influence tissue characteristics. The amount and volume of the mentioned parts can be different for different people, for example, some people have more fat and some have more bones. Therefore, because of the numerous parameters of a tissue, its overall evaluation can be complicated. Various papers have tried to consider it simple to examine human tissue. To be able to present a model of human tissue, first consider the basic conditions of the human being in a normal state, therefore, is assumed that the target tissue is human, disease-free, and aged between 30 and 50 years. To be qualified to obtain the dielectric constant of various parts of the tissue, its frequency must be known, because at different frequencies, different parts of the tissue show different behaviors. Table I shows the dielectric constant of different tissue parts of a normal human at a frequency of 3.2 GHz.

The tissue proposed in this paper is a human finger. The approximate dimensions for the index finger of a normal person with the described conditions are $4 \times 5 \times 10.5$ mm^3 and a schematic of its structure (four layers) is presented in Fig.1.

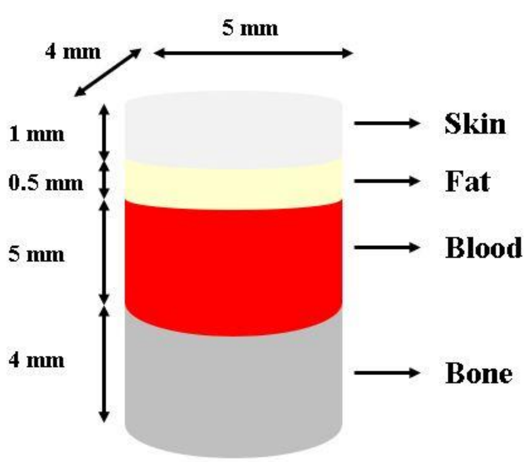

Fig. 1. Schematic of human index finger tissue.

TABLE I
The Dielectric Constant of Different Parts of Human Tissue in Frequency 3 GHz [26].

Tissue type	Dielectric constant
Skin	35
Fat	5.5
Blood	59
Bone	20

III. THE SENSOR DESIGNING

The planned sensor consists of three portions. The primary portion is a U-shaped arrangement. This part causes the microstrip structure to create a resonant frequency of 3.6GHz. The created resonance is not sharp and has a low Q-factor, which causes the sensor to be less sensitive when samples are measured. The second part consists of a waterfall structure, which is placed in the middle of the sensor and inside the U structure, and it causes the resonance to move slightly to a lower frequency and become sharper. Due to having parallel lines, this section creates capacitive coupling and can make the resonance sharper.

The second part consists of two interdigital structures, which are placed on both sides of the U-shaped structure, and cause the resonance to be exactly at a frequency of 3.2 GHz and increase its quality factor. Fig.2 and Table II indicate the designed sensor dimensions and Fig.3 shows the resonance frequency. Moreover, Fig.4 indicates the design steps of the suggested sensor along with its insertion loss.

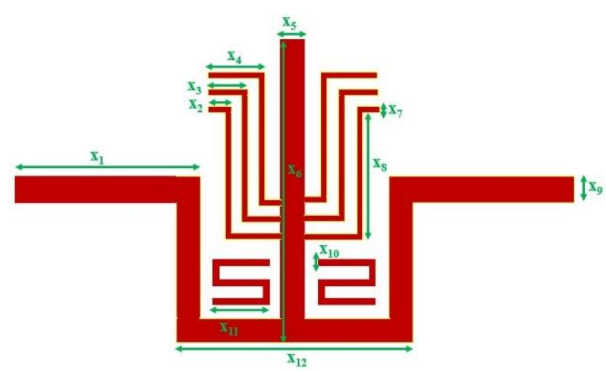

Fig. 2. The designed sensor dimensions.

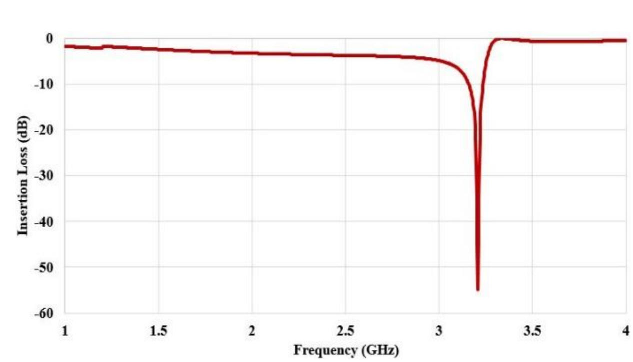

Fig. 3. The resonance frequency of the proposed sensor.

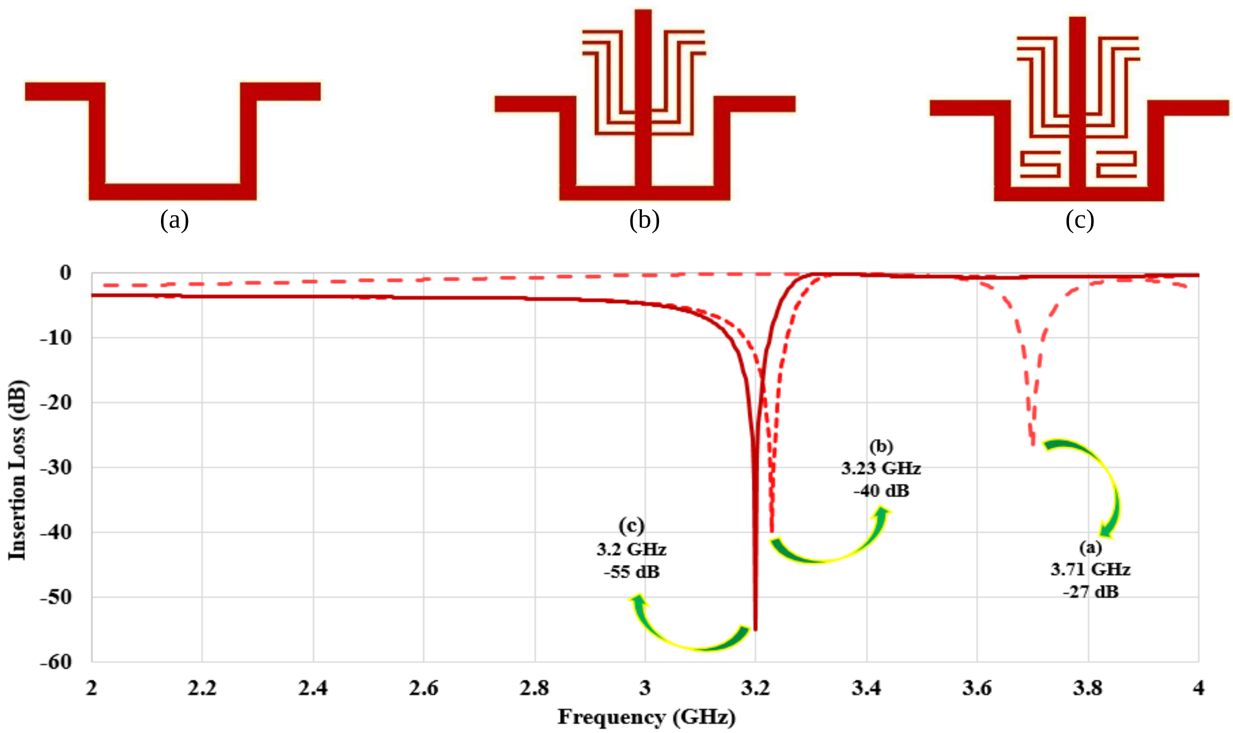

Fig. 4. The proposed sensor design steps a) the U-shaped structure b) adding the waterfall structure, c) adding two interdigital structures, and the final form and resonant frequencies of each step.

TABLE II
The Dimensions of the Designed Sensor.

Parameters	X_1	X_2	X_3	X_4	X_5	X_6
Length (mm)	11.2	1	1.8	2.6	1	9.2
Parameters	X_7	X_8	X_9	X_{10}	X_{11}	X_{12}
Length (mm)	0.5	3.2	1.2	0.3	2.95	10

IV. INVESTIGATION OF THE RESULTS OF BLOOD DIELECTRIC CHANGES ON THE SENSOR

For investigation of the status of the designed sensor, the third layer of the tissue model is considered, which is blood, and is considered as a variable. At frequency 3 GHz, its dielectric constant value is 59, and in the simulation, its value in 8 steps in values of 2 is increased, and each time the insertion loss of the sensor due to its contact with the sample is obtained. The simulation results are presented in Fig.5, also the measurement conditions and finger placement on the sensor are displayed in Fig.6.

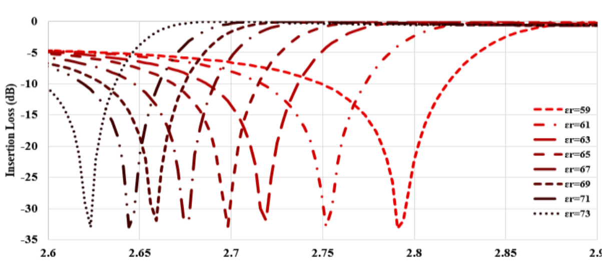

Fig. 5. The result of simulating blood changes in the tissue sample on the designed sensor.

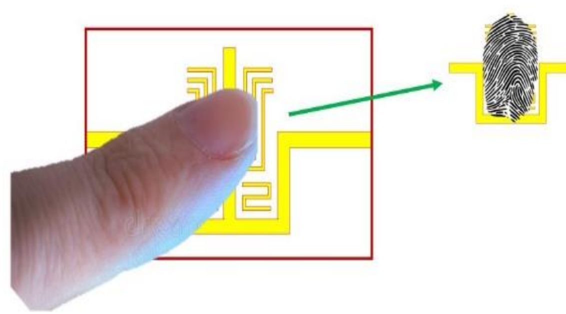

Fig. 6. The way the finger is placed on the sensor.

Formulas 1 and 2 display the calculating method of the quality factor and sensitivity, where f_0 is centre frequency and Δf is bandwidth. Moreover, f_{01} and f_{02} are the frequencies for the 1st and 2nd samples and $\Delta\varepsilon_r$ is the difference of their dielectric constant.

$$\text{Q-factor} = \frac{f_0}{\Delta f} \quad (1)$$

$$\text{Sensitivity} = \left|\frac{(f_{01} - f_{02})}{f_{01}} \frac{1}{\Delta\varepsilon_r}\right| \times 100\ (\%) \quad (2)$$

According to the obtained results and formulas 1 and 2, the quality factor and sensitivity of the proposed biosensor are equal to 5346 and 0.5%, respectively.

Table III displays a comparison between this work and prior research, and it can be understood that the obtained results are acceptable for the presented sensor.

TABLE III.
Comparison Between the Performance of the Proposed Sensor and Previously Reported Works.

Ref.	Freq. (GHz)	Q-factor	Sensitivity	Dimensions	Resonance Value
[4]	0.98	35	<0.17	16	> -6
[25]	4.8	30	<0.02	544	> -20
[37]	4.18	90	<0.03	1000	> -10
[50]	5.8	130	<0.24	1200	> -33
[51]	6.5	105	0.13	2500	> -33
[52]	2.4	5	0.28	1369	> -33
[53]	1.71	70	<0.019	8000	> -29
This work	3.2	5346	0.5	480	> -70

V. CONCLUSION

One of the diseases that the general public is facing is blood glucose. Therefore, they need to use an inexpensive tool that can quickly and accurately check blood glucose levels. Therefore, in this article, a microwave resonance sensor that can determine blood dielectric changes with high accuracy is designed. In the first part, a model of human finger tissue was used, which included skin, fat, blood, and bone, and the dielectric constant of each part was shown at the desired frequency. In the second part, a microwave sensor is designed and it is shown that when the tissue model makes contact with the proposed sensor, the sensor resonant frequency shifts due to the dielectric change of the third layer, which is blood. When the sample makes contact with the sensor, increasing the amount of blood dielectric, increases the tissue dielectric and the resonant frequency moves to lower values. The designed biosensor is used to investigate the different conditions in parts of the human tissue model, and due to the appropriate sensitivity of the planned biosensor, it can be used to test the inner layers of the tissue.

Acknowledgment

The authors acknowledge the Semnan University. Also, the authors would like to thank the editor, and reviewers for their constructive comments.

VI. REFERENCES

[1] Cuongab LT, Bang HT, Vy TT, Tien TQ. Digital subtraction angiography-guided ethanol sclerotherapy for peripheral venous malformation: A retrospective cohort study of single centre experience. Int. J. Surg. Open. 2022;42:100475.
[2] Liu W, Song KWJ, Zhang L, Liu Y. Ultralow friction of basil-based gel in the presence of ethanol as a green lubricant for biomedical applications. Tribol. Int. 2022;165:107320.
[3] Dogan H, Basyigit IB, Genc A. Determination and modelling of dielectric properties of the cherry leaves of varying moisture content over 3.30–7.05 GHz frequency range. J. microw. power electromagn. Energy. 2020;54(3):254-270.
[4] Dalgac S, Akdogan V, Kiris S, Incesu A, Akgol O, Unal E, Basar MT, Karaaslan M. Investigation of methanol contaminated local spirit using metamaterial based transmission line sensor. Measurement. 2021;178:109360-109370.
[5] Hamouleh-Alipour A, Khani S, Ashoorirad M, Baghbani R. Trapped multimodal resonance in magnetic field enhancement and sensitive THz plasmon sensor for toxic materials accusation. IEEE Sensors J. 2023; 13(2):14057-14066.
[6] Silva CCP, Bezerra MM, Morais SMA, Araujo JIL, Serres IJR, Silva JJ, Grilo MB, Neto JSDR. Non-invasive microwave sensor for ethanol content in gasoline applications. Instrum. Sci. Technol. 2019;1-6.
[7] Samanta S, Roy P, Kar P. Sensing of higher alcohols and selective sensing of iso-amyl alcohol by poly (o-phenylenediamine) nanofiber. IEEE Sens. J. 2020;20(16):8973-8980.
[8] Kiani S, Rezaei P, Navaei M, Abrishamian MS. Microwave sensor for detection of solid material permittivity in single/multilayer samples with high quality factor. IEEE Sens. J. 2018;18(24):9971-9982.
[9] Mehrjoo Z, Ebrahimi A, Ghorbani K. Microwave resonance-based reflective mode displacement sensor with wide dynamic range. IEEE Trans. Instrum. Meas. 2022;71:8000609.
[10] Khani S, Danaie M, Rezaei P. Plasmonic all-optical metal-insulator-metal switches based on silver nano-rods, comprehensive theoretical analysis and design guidelines. J. Computational Electron. 2021;20(1): 442-457.
[11] Kiani S, Rezaei P, Navaei M. Dual-sensing and dual-frequency microwave SRR sensor for liquid samples permittivity detection. Measurement. 2020;160:107805-107813.
[12] Yu C, Gong H, Zhang Z, Ni K, Zhao C. Temperature-compensated high-sensitivity relative humidity sensor based on band-pass filtering and vernier effect. IEEE Trans. Instrum. Meas. 2022;71:7001808.
[13] Zheng X, Jiang T. Triple notches bandstop microstrip filter based on archimedean spiral electromagnetic bandgap structure. Electronics. 2019;8(9):964-971.
[14] Navaei M, Rezaei P, Kiani S. A symmetric bar chart-shape microwave sensor with high Q-factor for permittivity determination of fluidics. Band-stop filter sensor based on SIW cavity for the non-invasive measuring of blood glucose. Int. J. Microw. Wirel. Technol. 2023;1-9.
[15] Zheng X, Pan Y, Jiang T. UWB bandpass filter with dual notched bands using T-shaped resonator and L-shaped defected microstrip structure. Micromachines. 2018;280(9):1-5.
[16] Cheng X, Hu J, Zhu K, Zhao Z. High-resolution polymer optical fibre humidity sensor utilizing single-passband microwave photonic filter. Measurement. 2021;179:109462-109472.
[17] Lio YT, Leung KW, Yang N. Compact absorptive filtering patch antenna. IEEE Trans. Antennas Propag. 2020;68(2):633-642.
[18] Nie HK, Xuan XW, Shi Q, Guo A, Li MJ, HJ L, Ren GJ. Wearable antenna sensor based on ebg structure for cervical curvature monitoring. IEEE Sens. J. 2022;22(1):315-323.
[19] Gharbi EM, Estrada MM, Garcia RF, Gil I. Determination of salinity and sugar concentration by means of a circular-ring monopole textile antenna-based sensor. IEEE Sens. J. 2021;21(21):23751-23760.
[20] Molina OO, Giraldo JD, Vera ER. Strain sensor based on rectangular microstrip antenna: numerical methodologies and experimental validation. IEEE Sens. J. 2021;21(20):22908-22917.
[21] Salek M, Celep M, Weimann T, Stokes D, Shang X, Phung GN, Kuhlmann K, Skinner J, Wang Y. Design, fabrication, and characterization of a d-band bolometric power sensor. IEEE Trans. Instrum. Meas. 2022;71:8002509.
[22] Wang F, Li H, Wang X, Ma T, Yu K, Lu Y, Zhang L, Liu Y. Temperature and curvature measurement based on low cavity loss flrd technology. IEEE Sens. J. 2022;22(3):2221-2228.
[23] Mohammadi P, Teimouri H, Mohammadi A, Demir S, Kara A. Dual band, miniaturized permittivity measurement sensor with

negative-order SIW resonator. IEEE Sens. J. 2021;21(20):22695-22724.
[24] Xu K, Chen C, Tang Y, Zhang X, Wu C, Geng M, Sun L. Improving the performance of all-solid-stated planar ph sensor with heat treated process. IEEE Sens. J. 2022;22(9):8410-8417.
[25] Velez P, Enano JM, Ebrahimi A, Herrojo C, Paredes F, Scott J, Ghorbani K, Martin F. Single-frequency amplitude-modulation sensor for dielectric characterization of solids and microfluidics. IEEE. Sens. Lett. 2021;21(10):12189-12201.
[26] Ji X, Luan N, Hou D, Zhang W, Jiang X, Zhang Z, Song L, Qi Y, Liu J. Sensitivity-tunable temperature spr sensor based on side-opening grapefruit fiber with liquid mixture. IEEE. Photon. J. 2022;14(3): 6823908.
[27] Sepulveda HVL, Cervantes JLO, Saavedra CE. Multifrequency coupled-resonator sensor for dielectric characterization of liquids. IEEE Trans. Instrum. Meas. 2021;70:1-15.
[28] Kompella PLS, Sudha RG. Two-channel dual-band microwave EBG sensor for simultaneous dielectric detection of liquids. Int. J. Electron. Commun. 2022;146:154099-154107.
[29] Sorocki J, Wincza K, Gruszczynski S, Piekarz I. Direct broadband dielectric spectroscopy of liquid chemicals using microwave-fluidic two-wire transmission line sensor. IEEE Trans. Microwave Theory Tech. 2021;269(17):2569-2578.
[30] Khani S, et al. Adjustable compact dual-band microstrip bandpass filter using T-shaped resonators. Microw. Opt. Technol. Lett. 2017;59(12): 2970-2975.
[31] Kiani S, Rezaei P. Microwave substrate integrated waveguide resonator sensor for non-invasive monitoring of blood glucose concentration: Low cost and painless tool for diabetics. Measurement. 2023;219: 113232.
[32] Fu L, Huang J, Xiang Y, Chen Y, Gu W, Wu Y. A miniaturized differential microwave microfluidic sensor with high decoupling. IEEE. Microw. Wirel. Compon. Lett. 2021;31(7):909-912.
[33] Puyol R, Pétré S, Danlée Y, Walewyns T, Francis LA, Flre D. An ultra-low-power read-out circuit for interfacing novel gas sensors matrices. IEEE Sens. J. 2022;22(10):9521-9533.
[34] Herrojo C, Velez P, Enano JM, Su L, Casacuberta P, Gil M, Martin F. Highly sensitive defect detectors and comparators exploiting port imbalance in rat-race couplers loaded with step-impedance open-ended transmission lines. IEEE Sens. J. 2021;21(23):26731-26733.
[35] Kiani S, Rezaei P, Karami M, Sadeghzadeh RA. Substrate integrated waveguide quasi-elliptic bandpass filter with parallel coupled microstrip resonator. Electron. Lett. 2018;54(10):667-668.
[36] Su L, Enano JM, Velez P, Casacuberta P, Gil M, Martin F. Phase-variation microwave sensor for permittivity measurements based on a high-impedance half-wavelength transmission line. IEEE. Sens. Lett. 2021;21(9):10647-10656.
[37] Nguyen KT, Tseng CH. A new microwave humidity sensor with near-field self-injection-locked technology. IEEE Sens. J. 2021;21(19):21520-21528.
[38] Kiani S, Rezaei P, Fakhr M. Dual-frequency microwave resonant sensor to detect non-invasive glucose level changes through the fingertip. IEEE Trans. Instrum. Measurement. 2021;70:6004608.
[39] Cai C, Wei L, Wu X, Wang D. A novel gradient thermoelectric microwave power sensors based on gaas mmic technology. Microsyst. Technol. 2021;27:243–249.
[40] Bag B, Mondal K, Sarkar PP. Dual-band dual-sense broadband circularly polarized parasitic ring loaded monopole antenna for satellite applications. Int. J. Commun. Syst. 2022;1-1.
[41] Kumar S, Kumar M, Singh A. Exploiting WiMAX for covert transmission of secret data over fading channel. Int. J. Commun. Syst. 2020;33(8):1-9.
[42] Mohammadi S, Adhikari KK, Jain MC, Zarifi MH. High-resolution, sensitivity-enhanced active resonator sensor using substrate-embedded channel for characterizing low-concentration liquid mixtures. IEEE Trans. Microwave Theory Tech. 2021;70(1):576-586.
[43] Li T, Shang H, Wang B, Mao C, Wang W. High-pressure sensor with high sensitivity and high accuracy for full ocean depth measurements. IEEE Sens. J. 2022;22(5):3994-4003.
[44] Yazdi F, Nikzamir A, Mealy T, Nada MY, Capolino F. Triple ladder lumped circuit with sixth order modal exceptional degeneracy. IEEE. Trans. Circuits. Syst. I. Regul. Pap. 2022;69(5):1910-1918.
[45] Xue F, Adedokun G, Xie D, Liu R, Zhang Y, Muhammad M, Xu L, Wu F. A low power four-channel metal oxide semiconductor gas sensor array with t-shaped structure. J. Microelectromech. Syst. 2022;31(2): 275-282.
[46] Khani S, Hayati M. Optical biosensors using plasmonic and photonic crystal band-gap structures for the detection of basal cell cancer. Sci. Rep. 2022;12(1):1-19.
[47] Khani S, Hayati M. Optical sensing in single-mode filters base on surface plasmon H-shaped cavities. Opt. Commun. 2022;505:127534.
[48] Khani S, Hayati M. An ultra-high sensitive plasmonic refractive index sensor using an elliptical resonator and MIM waveguide. Superlattices Microstruct. 2021;156:106970.
[49] Khani S, Danaie M, Rezaei P, Shahzadi A. Compact ultra-wide upper stopband microstrip dual-band BPF using tapered and octagonal loop resonators. Frequenz. 2020;74(1-2):61-71.
[50] Jain S, Tiwari NK, Akhtar MJ. CSIWC RF sensor for micro-fluidic non-contact quality assessment of milk. Int. J. RF Microw. Comput. Aided Eng. 2021;32(2):1-9.
[51] Zhang X, Ruan C, Wang W, Cao Y. Submersible high sensitivity microwave sensor for edible oil detection and quality analysis. IEEE Sens. J. 2021;21(12):13230-13238.
[52] Harnsoongnoen S. Metamaterial-inspired microwave sensor for detecting the concentration of mixed phosphate and nitrate in water. IEEE Trans. Instrum. Meas. 2021;70:1-8.
[53] Appusamy S, Krishnan S, Gopikrishna M, Raman S. Bio-based materials for microwave Devices: a review. J. Electron. Mater. 2021;50:1893-1901.